

Magnetotransport properties of FeSe in fields up to 50 T.

Y.A. Ovchenkov^{a,*}, D.A. Chareev^{b,c,d}, V.A. Kulbachinskii^a, V.G. Kytin^a,
D.E. Presnov^{a,e}, Y. Skourski^f, O.S. Volkova^{a,c,g}, A.N. Vasiliev^{a,g,h}

^a*Faculty of Physics, M.V. Lomonosov Moscow State University, Moscow 119991, Russia*

^b*Institute of Experimental Mineralogy RAS, Chernogolovka, Moscow District, 142432, Russia*

^c*Ural Federal University, 620002 Ekaterinburg, Russia*

^d*Kazan Federal University, 18 Kremlyovskaya Str., Kazan, 420008, Russia*

^e*Skobeltsyn Institute of Nuclear Physics, Moscow 119991, Russia*

^f*Dresden High Magnetic Field Laboratory (HLD-EMFL), HZDR, Dresden, Germany*

^g*National University of Science and Technology MISiS, 119049 Moscow, Russia*

^h*National Research South Ural State University, 454080 Chelyabinsk, Russia*

Abstract

Magnetotransport properties of the high-quality FeSe crystal, measured in a wide temperature range and in magnetic fields up to 50 T, show the symmetry of the main holelike and electronlike bands in this compound. In addition to the main two bands, there is also a tiny, highly mobile, electronlike band which is responsible for the non-linear behavior of $\rho_{xy}(B)$ at low temperatures and some other peculiarities of FeSe. We observe the inversion of the ρ_{xx} temperature coefficient at a magnetic field higher than about 20 T which is an implicit conformation of the electron-hole symmetry in the main bands.

Keywords: High-Tc superconductors, Galvanomagnetic effects, Electronic band structure

PACS: 74.70.Xa, 72.15.Gd, 74.25.F-, 71.20.-b

1. Introduction

FeSe is a very important and interesting superconducting material with complicated electronic and transport properties [1]. It is a nearly compen-

*Corresponding author

Email address: ovtchenkov@mig.phys.msu.ru (Y.A. Ovchenkov)

sated semimetal with low carrier concentration. For the physics of superconductivity, it is a new type of superconducting materials and it is a new playground to test out the existing theories of superconductivity. In particular, the low carrier concentration should have allowed a significant variation of a superconducting transition temperature (T_c) under variation of a carrier concentration. Indeed, it is demonstrated that the transition temperature can be substantially varied using a gate electrode [2]. However the pairing mechanism in FeSe and other iron-based superconductors is still being debated, and the reasons, causing a T_c increase under pressure [3], and for a mono-layer FeSe film on an epitaxial substrate [4], are unclear.

The properties of FeSe, as well as many other iron-based superconductors, can not be described by a simple two-band semimetal model. The first studies of the iron-based superconductors revealed multiband effects and electron-hole asymmetry in $\text{Ba}(\text{FeCo})_2\text{As}_2$ [5]. Later, an analysis of the magnetic field dependence of ρ_{xy} and ρ_{xx} suggested the presence of the highly mobile electronlike band in BaFe_2As_2 [6]. The similar highly mobile band exists in many other iron-based superconductors including FeSe family [7] and, apparently, originates from a small local region of the Fermi surface. Since the mobilities of the two main bands are several times lower than for the highly mobile band, their properties can be studied separately in a high magnetic field where the conductivity of the highly mobile band is suppressed significantly.

Here we report the magnetotransport properties of the high-quality FeSe crystal measured in a wide temperature range and magnetic fields up to 50 T. The obtained data prove a good symmetry of the main electronlike and holelike bands. A remarkable phenomenon is observed at temperatures below 100 K. All $\rho_{xx}(B)$ curves, corresponding to different temperatures, cross each other in the region 15-20 T and 0.1-0.15 m Ω cm. Therefore, a crossover from a metallic-type $\rho_{xx}(T)$ to a semiconductor-type dependence occurs at a magnetic field higher than 20 T. Such behavior has a simple description within the two-band model which gives another way to extract the parameters of the main bands.

2. Experiment

The FeSe crystals were grown using the KCl/AlCl_3 flux technique [8]. The chemical composition of the crystals was studied with the energy dispersive

micro analysis system. The composition measurements were done at three points for four average size crystals.

Electrical measurements were done on a cleaved rectangular sample with lengths of 1.2 mm, widths 0.6 mm and thicknesses about 0.05 mm. Contacts were made by sputtering of Au/Ti layers through a precisely machined mechanical mask. The current electrodes were 0.1 mm wide lines along small sides of the bar. Potential and Hall $0.1 \times 0.1 \text{ mm}^2$ electrodes were connected to a sample holder with a 0.025 mm gold wire using H20E silver epoxy.

DC magnetoresistance and Hall effect measurements were done using EDC options of Quantum Design MPMS 7T with Keithley 2400 and Keithley 2182A. Measurements of resistance in pulsed magnetic fields up to 50 T were done in HLD at HZDR, Germany.

3. Results and discussion

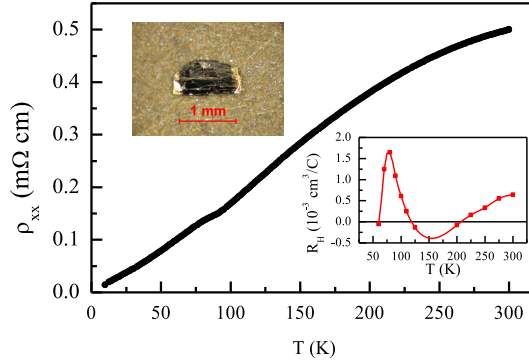


Figure 1: The temperature dependence of the resistivity ρ_{xx} . Top inset: the picture of the investigated crystal. Bottom inset: Temperature dependence of the Hall coefficient R_H .

The temperature dependence of the sample resistance is shown in Fig.1. The anomaly at $\rho_{xx}(T)$ around 90 K corresponds to the structural phase transition. The resistivity at 15 K is 22 times lower than at 300 K which indicates a high quality of used crystal. An optical image of the studied crystal is shown in the top inset of Fig.1. The bottom inset of Fig.1 shows the temperature dependence of the Hall coefficient R_H . The Hall coefficient has sign reversal points in presented temperature range which is one of the

consequences of a carrier compensation. The low-temperature behavior of R_H is not plotted because of non-linearity of $\rho_{xy}(B)$ at low temperatures. The quality of the sample is also confirmed by $R(T, B)$ measurements near

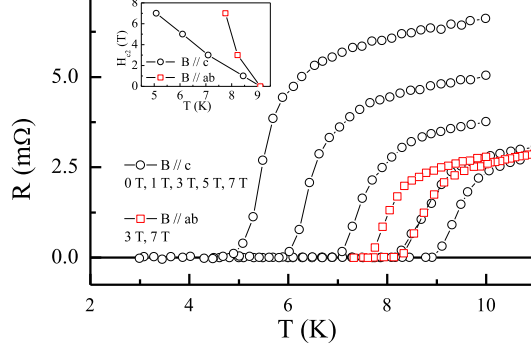


Figure 2: The temperature dependence of the resistance near a superconducting transition at the various magnetic fields. Inset: Temperature dependence of H_{C2} critical field for the two field orientations.

the superconducting transition temperature. Figure 2 shows $R(T)$, measured around the transition, in magnetic fields parallel and perpendicular to the crystal plane. The inset shows the temperature dependencies of the critical fields for these two orientations determined at zero-resistivity points. The ratio of slopes for these dependencies is 3.1-3.4. It is the ratio of coherence lengths for the ab plane and for the c axis direction. This value of anisotropy is close to the highest reported for FeSe single crystals which confirms a perfect layered structure of the studied crystal.

The field dependence of the resistivity tensor components within a quasi-classical relaxation-time approximation can be expressed as a sum of l band terms:

$$\sigma_{xx} = \sum_{i=1}^l \frac{\sigma_i}{(1 + \mu_i^2 B^2)} \quad (1)$$

$$\sigma_{xy} = \sum_{i=1}^l \frac{s_i \sigma_i \mu_i B}{(1 + \mu_i^2 B^2)} \quad (2)$$

$$\sigma_i = en_i \mu_i \quad (3)$$

where σ_{xx} and σ_{xy} are conductivity tensor components, i is a band index,

σ_i , μ_i , and n_i are absolute values of a band conductivity, a carrier mobility and a concentration correspondingly; s_i is "-1" for a hole and "+1" for an electron bands. Resistivity tensor components ρ_{xx} and ρ_{xy} in a tetragonal crystal are related as follows:

$$\rho_{xx} = \rho_{yy} = \frac{\sigma_{xx}}{(\sigma_{xx}^2 + \sigma_{xy}^2)} \quad (4)$$

$$-\rho_{xy} = \rho_{yx} = \frac{\sigma_{xy}}{(\sigma_{xx}^2 + \sigma_{xy}^2)} \quad (5)$$

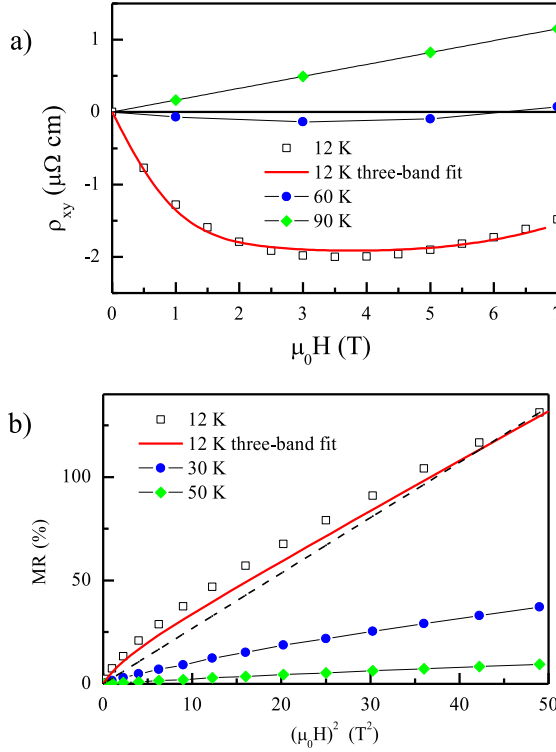


Figure 3: (a) The field dependence of ρ_{xy} . (b) Magnetoresistance $MR = (\rho_{xy}(B) - \rho_{xy}(0))/\rho_{xy}(0)$ versus B^2 . The straight dash line in (b) highlights the curvature of the 12 K curve. The experimental data at 12 K are fitted with the three-band model.

For the two-band material, this model gives a linear in B law for ρ_{xy} and B^2 for ρ_{xx} in the limit $\mu_i B \ll 1$ for both mobilities. The measured depen-

dencies $\rho_{xy}(B)$ and magnetoresistance $MR(B) = (\rho_{xx}(B) - \rho_{xx}(0))/\rho_{xx}(0)$ in dependence on B^2 are shown in Fig. 3 a) and b) respectively. It is clearly seen that the curves corresponding 12 K deviate substantially from a linear dependence. A similar behavior was reported for many iron-based superconductors and can be described within the three-band model by adding to a couple of main electron and hole bands, which have almost the same concentrations and mobilities, the tiny band with appreciably higher mobility [7]. The Table 1 lists the results of the simultaneous fit of $\sigma_{xy}(B)$ and $\sigma_{xx}(B)$ data, obtained at 12 K and 30 K, with three-band equations (1) - (3). The ratios n_e/n_h and μ_e/μ_h at 12 K are 0.84 and 1.12 respectively. Therefore, in a quasiclassical relaxation-time approximation FeSe can be described as having the two main electron and hole bands, with approximately equal values of a concentration and a mobility, and a tiny mobile band with a 3-5 % of the total carrier concentration which provide about 10-15 % of the total conductivity in zero fields. The relative contribution to the total conductivity of this highly mobile band rapidly decreases with increasing magnetic field. For example, accordingly the data listed in Table 1 the band e_2 provides 13% of the total conductivity at 12 K in zero field and only about 2% in 5 T.

Table 1: The results of the simultaneous fitting of $\sigma_{xy}(B)$ and $\sigma_{xx}(B)$ in field range up to 7 T using the three-band model.

<i>band</i>	12 K		30 K	
	<i>n</i> (10^{19} cm^{-3})	μ (cm^2/Vs)	<i>n</i> (10^{19} cm^{-3})	μ (cm^2/Vs)
e_1	8.98	1537	8.4	670
h_1	10.67	1365	10.5	615
e_2	0.66	6481	0.6	2500

Consequentially, in high magnetic fields a two-band semimetal is a good model to describe the FeSe transport properties. It allows to give a simple explanation for a crossover to a negative temperature coefficient of ρ_{xx} in high magnetic fields which is demonstrated in Fig. 4. This figure shows $\rho_{xx}(B)$ corresponding to temperatures in the range 30-80 K. All curves cross each other in the field range 15-25 T. Therefore, the temperature coefficient of resistivity ρ_{xx} changes it's sign from a positive in low magnetic fields to a negative in high magnetic fields. The inset of Fig.4 shows $\rho_{xx}(T)$ at zero and 45 T magnetic fields which confirm this inversion.

To get a clear and comprehensive expression, we consider the simplest

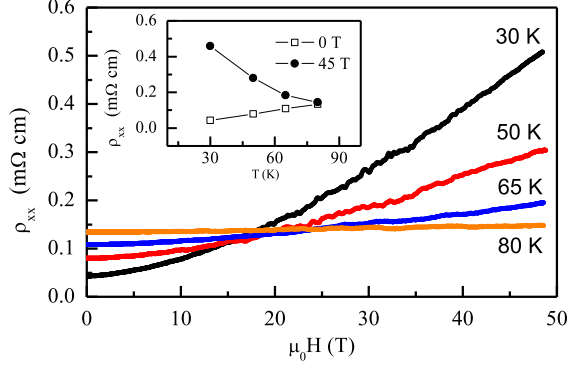


Figure 4: Field dependence of the resistivity ρ_{xx} at temperatures from 30 to 80 K. Inset : The temperature dependence of ρ_{xx} at 0 and 45 T.

possible two-band model with the equal values of the electron and hole concentrations and mobilities: $n_e = n_h = n_0/2$, $\mu_e = \mu_h = \mu_0$, and consequently $\sigma_e = \sigma_h = \sigma_0/2$. Substitution in (1) and (2) gives:

$$\sigma_{xx} = \sum_{i=e,h} \frac{\sigma_i}{(1 + \mu_i^2 B^2)} = \frac{\sigma_0}{(1 + \mu_0^2 B^2)} \quad (6)$$

$$\sigma_{xy} = \sum_{i=e,h} \frac{s_i \sigma_i \mu_i B}{(1 + \mu_i^2 B^2)} = 0 \quad (7)$$

Eq. (4) reduces to:

$$\rho_{xx} = 1/\sigma_{xx} = \frac{1}{\sigma_0} (1 + \mu_0^2 B^2); \quad (8)$$

therefore MR has simple expression:

$$MR = \mu_0^2 B^2 \quad (9)$$

Eq. (8) can be written as follows:

$$\rho_{xx} = \frac{1}{en_0\mu_0} + \frac{\mu_0}{en_0} B^2 \quad (10)$$

and we can introduce:

$$\rho_0 = \frac{1}{en_0\mu_0} = \frac{1}{en_0} \mu_0^{-1} \quad (11)$$

$$\rho_B = \frac{\mu_0}{en_0} B^2 = \frac{B^2}{en_0} \mu_0 \quad (12)$$

where ρ_0 and ρ_B are independent and dependent on magnetic field terms respectively. It is clearly seen that temperature dependencies of these terms, which are due to temperature dependence of μ_0 , are reciprocal. Therefore, if in a zero magnetic field $\rho_{xx}(T) = f(T)$, where $f(x)$ - any arbitrary function, then in a strong enough magnetic field B :

$$\rho_{xx}(T) \approx \left(\frac{B}{en_0}\right)^2 f^{-1}(T); \quad (13)$$

This simple and interesting phenomenon is exactly what observed for FeSe. It allows to find the carrier concentration from the relation:

$$(\rho_{xx}(B) - \rho_{xx}(0))\rho_{xx}(0) = \left(\frac{B}{en_0}\right)^2 \quad (14)$$

If μ_1 and μ_2 are the mobility values at temperatures T_1 and T_2 , then intersection at B_x gives the next equation:

$$\frac{1}{en_0\mu_1} + \frac{\mu_1}{en_0}B_x^2 = \frac{1}{en_0\mu_2} + \frac{\mu_2}{en_0}B_x^2 \quad (15)$$

The solution of Eq. (15) is:

$$B_x^2 = \frac{1}{\mu_1\mu_2} \quad (16)$$

Using obtained relations we can determine "the experimental" values of the band's parameters. At 30 K $\rho_{xx}(0)=4.28 \times 10^{-5} \Omega\text{cm}$ and $\rho_{xx}(45T)=4.59 \times 10^{-4} \Omega\text{cm}$. For these values the equation (14) gives $2.16 \times 10^{20} \text{ cm}^{-3}$ for carrier concentration and (9) gives 600 (cm^2/Vs) for carrier mobility. These values are in a good agreement the values listed in Table 1. From equation (16) it follows that $\rho_{xx}(B)$ curves for the temperature range corresponding the mobility range $[\mu_1, \mu_2]$ will cross each other in the field range $[1/\mu_1, 1/\mu_2]$. It gives again about 600-700 (cm^2/Vs) for the mobility value at 30 K. In general, it shows that the magnetotransport properties of FeSe can be satisfactory quantitatively described within the quasiclassical approximation. Reported violation of the Kohler's rule for these compounds [9] probably related to the variation of the highly mobile band parameters.

The data in Table 1 show a good symmetry of the main electron and hole band parameters. These data were obtained from the transport measurements up to fields satisfying relation $\mu B \approx 1$ for the main bands. To

improve the accuracy of comparison and to probe the carriers properties in higher fields we fitted the $\rho_{xx}(B)$ dependence measured at 1.5 K (see Fig. 5) with explicit two band expression for MR [10]:

$$MR = \frac{\alpha B^2}{(1 + \beta B^2)} \quad (17)$$

$$\alpha = \sigma_e \sigma_h (\mu_e + \mu_h)^2 / (\sigma_e + \sigma_h)^2 \quad (18)$$

$$\beta = (\mu_e \mu_h (n_e - n_h))^2 / (\sigma_e + \sigma_h)^2 \quad (19)$$

where α is a slope of $\rho_{xx}(B^2)$ in low fields and β describes a saturation of $\rho_{xx}(B^2)$. The ratio β/α is:

$$\frac{\beta}{\alpha} = \frac{\mu_e \mu_h}{(\mu_e + \mu_h)^2} \frac{(n_e - n_h)^2}{n_e n_h} \quad (20)$$

The coefficient β allows to determine an exact value of the non-compensation $|(n_e - n_h)|$.

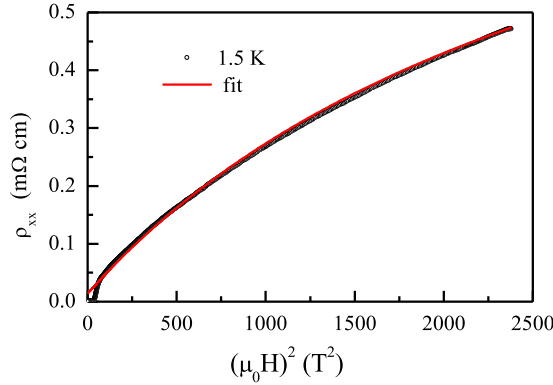


Figure 5: Experimental dependence of ρ_{xx} at 1.5 K and fitting function $\rho_{1.5} \times (1 + MR)$ for $\rho_{1.5} = 1.42 \times 10^{-5} \Omega \text{cm}$ and MR expressed in Eq. (17) with $\alpha = 2.43 \times 10^{-2} (\text{T}^{-2})$, and $\beta = 3.3 \times 10^{-4} (\text{T}^{-2})$.

For the almost symmetrical $n_e \approx n_h = n_0/2$, $\mu_e \approx \mu_h = \mu_0$, and $\sigma_e \approx \sigma_h = \sigma_0/2$. Then $\alpha \approx \mu_e \mu_h \approx \mu_0^2$ and $\beta/\alpha \approx ((n_e - n_h)/n_0)^2$. Then the slope of $\rho_{xx}(B^2)$, which is equal to $2.43 \times 10^{-2} (\text{T}^{-2})$, gives for mobility values, if, suppose, they are equal, about $1560 (\text{cm}^2/\text{Vs})$. It is the same value as it were determined for the main bands at 12 K (see Table 1) which can be explained by a mobility saturation at low temperatures. The ratio β/α is 1.36×10^{-2}

then $|(n_e - n_h)|/n_0$ is about 0.11 which gives $(n_e/n_h = 1.22$ or 0.82 . The last value is in a good agreement with 0.84 which was previously obtained for data in Table 1.

4. Conclusion

The experimental data on the transport properties of the high-quality FeSe crystal in high magnetic fields show a good symmetry of the main electron and hole bands. In particular, this symmetry allows observing the inversion of the temperature coefficient of resistivity. The properties of the tiny highly mobile band deserve a further investigation because of it can be responsible for the measurable interaction of ultrasound with electrons observed in FeSe [11] and, therefore, can play a special role in an appearance of superconductivity in this compound.

5. Acknowledgments

This work was supported by the Ministry of Education and Science of the Russian Federation in the framework of Increase Competitiveness Program of NUST MISiS project K2-2016-066, by the Russian Government Program of Competitive Growth of Kazan Federal University and by Act 211 of Government of the Russian Federation, contracts 02.A03.21.0004, 02.A03.21.0006 and 02.A03.21.0011. We acknowledge support of Russian Foundation for Basic Research through Grants of-m-16-29-03266, 15-03-99628. We acknowledge the support of HLD at HZDR, a member of the European Magnetic Field Laboratory (EMFL).

References

- [1] A. I. Coldea, M. D. Watson, The key ingredients of the electronic structure of FeSe, ArXiv e-prints [arXiv:1706.00338](https://arxiv.org/abs/1706.00338).
- [2] B. Lei, J. H. Cui, Z. J. Xiang, C. Shang, N. Z. Wang, G. J. Ye, X. G. Luo, T. Wu, Z. Sun, X. H. Chen, Evolution of high-temperature superconductivity from a low- T_c phase tuned by carrier concentration in fese thin flakes, *Phys. Rev. Lett.* 116 (2016) 077002. doi:10.1103/PhysRevLett.116.077002.
URL <https://link.aps.org/doi/10.1103/PhysRevLett.116.077002>

- [3] S. Medvedev, T. M. McQueen, I. A. Troyan, T. Palasyuk, M. I. Erements, R. J. Cava, S. Naghavi, F. Casper, V. Ksenofontov, G. Wortmann, C. Felser, Electronic and magnetic phase diagram of [beta]-Fe_{1.01}Se with superconductivity at 36.7 K under pressure, *Nat Mater* 8 (8) (2009) 630–633. doi:10.1038/nmat2491.
URL <http://dx.doi.org/10.1038/nmat2491>
- [4] W. Qing-Yan, L. Zhi, Z. Wen-Hao, Z. Zuo-Cheng, Z. Jin-Song, L. Wei, D. Hao, O. Yun-Bo, D. Peng, C. Kai, W. Jing, S. Can-Li, H. Ke, J. Jin-Feng, J. Shuai-Hua, W. Ya-Yu, W. Li-Li, C. Xi, M. Xu-Cun, X. Qi-Kun, Interface-induced high-temperature superconductivity in single unit-cell FeSe films on SrTiO₃, *Chinese Physics Letters* 29 (3) (2012) 037402.
URL <http://stacks.iop.org/0256-307X/29/i=3/a=037402>
- [5] L. Fang, H. Luo, P. Cheng, Z. Wang, Y. Jia, G. Mu, B. Shen, I. I. Mazin, L. Shan, C. Ren, H.-H. Wen, Roles of multiband effects and electron-hole asymmetry in the superconductivity and normal-state properties of Ba(Fe_{1-x}Co_x)₂As₂, *Phys. Rev. B* 80 (2009) 140508. doi:10.1103/PhysRevB.80.140508.
URL <https://link.aps.org/doi/10.1103/PhysRevB.80.140508>
- [6] S. Ishida, T. Liang, M. Nakajima, K. Kihou, C. H. Lee, A. Iyo, H. Eisaki, T. Kakeshita, T. Kida, M. Hagiwara, Y. Tomioka, T. Ito, S. Uchida, Manifestations of multiple-carrier charge transport in the magnetotransportally ordered phase of BaFe₂As₂, *Phys. Rev. B* 84 (2011) 184514. doi:10.1103/PhysRevB.84.184514.
URL <http://link.aps.org/doi/10.1103/PhysRevB.84.184514>
- [7] Y. A. Ovchinnikov, D. A. Chareev, V. A. Kulbachinskii, V. G. Kytin, D. E. Presnov, O. S. Volkova, A. N. Vasiliev, Highly mobile carriers in iron-based superconductors, *Superconductor Science and Technology* 30 (3) (2017) 035017.
URL <http://stacks.iop.org/0953-2048/30/i=3/a=035017>
- [8] D. Chareev, E. Osadchii, T. Kuzmicheva, J.-Y. Lin, S. Kuzmichev, O. Volkova, A. Vasiliev, Single crystal growth and characterization of tetragonal Fe_{1-x} superconductors, *CrystEngComm* 15 (2013) 1989–1993. doi:10.1039/C2CE26857D.
URL <http://dx.doi.org/10.1039/C2CE26857D>

- [9] T. Terashima, N. Kikugawa, S. Kasahara, T. Watashige, Y. Matsuda, T. Shibauchi, S. Uji, Magnetotransport study of the pressure-induced antiferromagnetic phase in fese, Phys. Rev. B 93 (2016) 180503. doi: 10.1103/PhysRevB.93.180503.
URL <https://link.aps.org/doi/10.1103/PhysRevB.93.180503>
- [10] J. S. Kim, A matrix formulation of magnetoresistance for an arbitrary j-fold multicarrier semiconductor system via the reduced-conductivity-tensor scheme in the nonquantizing regime, Journal of Applied Physics 84 (1) (1998) 292–300. arXiv:<http://dx.doi.org/10.1063/1.368026>, doi:10.1063/1.368026.
URL <http://dx.doi.org/10.1063/1.368026>
- [11] G. A. Zvyagina, T. N. Gaydamak, K. R. Zhekov, I. V. Bilich, V. D. Fil, D. A. Chareev, A. N. Vasiliev, Acoustic characteristics of fese single crystals, EPL (Europhysics Letters) 101 (5) (2013) 56005.
URL <http://stacks.iop.org/0295-5075/101/i=5/a=56005>

List of Figures

- | | | |
|---|--|---|
| 1 | The temperature dependence of the resistivity ρ_{xx} . Top inset: the picture of the investigated crystal. Bottom inset: Temperature dependence of the Hall coefficient R_H | 3 |
| 2 | The temperature dependence of the resistance near a superconducting transition at the various magnetic fields. Inset: Temperature dependence of H_{C2} critical field for the two field orientations. | 4 |
| 3 | (a) The field dependence of ρ_{xy} . (b) Magnetoresistance $MR = (\rho_{xy}(B) - \rho_{xy}(0))/\rho_{xy}(0)$ versus B^2 . The straight dash line in (b) highlights the curvature of the 12 K curve. The experimental data at 12 K are fitted with the three-band model. . . | 5 |
| 4 | Field dependence of the resistivity ρ_{xx} at temperatures from 30 to 80 K. Inset : The temperature dependence of ρ_{xx} at 0 and 45 T. | 7 |
| 5 | Experimental dependence of ρ_{xx} at 1.5 K and fitting function $\rho_{1.5} \times (1 + MR)$ for $\rho_{1.5}=1.42 \times 10^{-5} \Omega\text{cm}$ and MR expressed in Eq. (17) with $\alpha=2.43 \times 10^{-2} (\text{T}^{-2})$, and $\beta=3.3 \times 10^{-4} (\text{T}^{-2})$. . . | 9 |